

GEM: Generative Supervision Helps Embodied Intelligence

Ruowen Zhao¹, Bangguo Li¹, Zuyan Liu^{1,2,†}, Yanan Liang¹, Junliang Ye¹, Fangfu Liu¹,
Diankun Wu¹, Zhengyi Wang¹, Xumin Yu², Yongming Rao^{2,‡}, Han Hu², Jun Zhu^{1,‡}

¹ Tsinghua University ² Tencent Hunyuan

Abstract

Embodied Vision-Language Models (VLMs) have demonstrated impressive performance and generalization in robotics, particularly within Vision-Language-Action frameworks. However, a significant gap remains between the high-level semantic focus of standard text-guided pre-training paradigms and the low-level spatial and physical knowledge critical for execution in embodied environments. In this paper, we introduce **GEM**, a Generative-supervised Embodied vision-language Model designed to bridge this divide. We propose integrating a depth map generation task directly into the VLM pre-training phase. By training this generative objective jointly with the main model, we observe substantial improvements in embodied intelligence, significantly enhancing both semantic understanding and physical operation capabilities. To support this paradigm, we curate and release GEM-4M, a comprehensive large-scale dataset featuring a mixture of grounding, reasoning, and planning data paired with high-quality depth supervision. Extensive experiments demonstrate that GEM achieves state-of-the-art results across diverse embodied benchmarks. Furthermore, our deployed action model, GEM-VLA, exhibits vastly superior task execution abilities in both simulation environments and real-world evaluations. Code, models, and datasets are available at <https://zhaorw02.github.io/GEM/>.

Keywords: Embodied Intelligence · Vision-Language Models · Vision-Language-Action Models

1 Introduction

Recent advancements in Vision-Language Models (VLMs) (Bai et al., 2025; Wang et al., 2025a; Li et al., 2024a; Beyer et al., 2024; Liu et al., 2023b) have unlocked remarkable capabilities in embodied understanding, encompassing critical skills such as spatial recognition, physical grounding, and complex task planning. By effectively aligning visual perception with natural language reasoning, these models (Yang et al., 2025b; Hao et al., 2025b; Ji et al., 2025; Liu et al., 2025a) have emerged as robust foundation architectures for Vision-Language-Action (VLA) frameworks (Kim et al., 2024; Intelligence et al., 2025b; Team et al., 2024; Brohan et al., 2022). Consequently, Embodied VLMs are increasingly being leveraged to drive a massive array of downstream operational tasks, demonstrating potential for generalization and autonomous execution within dynamic, real-world physical environments.

[†] Project Lead. [‡] Corresponding author.

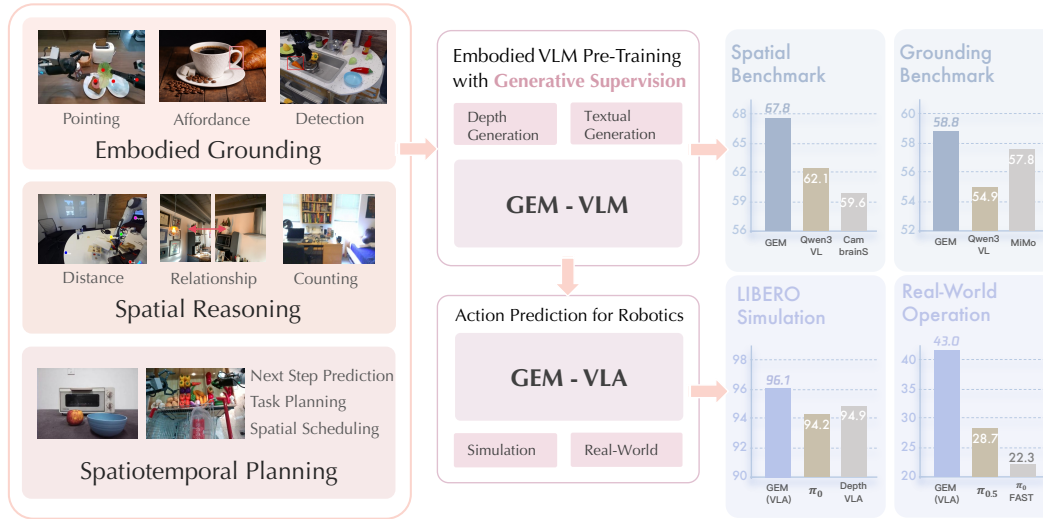


Fig. 1: **Overview of GEM.** GEM is a generative-supervised embodied VLM that strengthens semantic reasoning and physical grounding by combining language modeling with an auxiliary depth-generation objective (center). Trained on the high-quality, large-scale pre-training datasets spanning diverse embodied tasks (left), GEM achieves strong performance across a wide range of embodied benchmarks. Based on the architecture of GEM, the extending GEM-VLA attains state-of-the-art success rates on LIBERO and generalizes well to real-world robot manipulation (right).

Despite these foundational successes, the predominant paradigm for training embodied VLMs (Ji et al., 2025; Yang et al., 2025b; Dang et al., 2026; Hao et al., 2025b; Azzolini et al., 2025) relies heavily on scaling up massive visual question answering datasets (Seraman et al., 2024; Yuan et al., 2024; Yang et al., 2025b; Qu et al., 2025b; Chen et al., 2025b). While this approach effectively boosts performance on high-level semantic benchmarks and passive comprehension tasks (Zhou et al., 2025; Yuan et al., 2024; Song et al., 2025a; Tong et al., 2024; Yang et al., 2024), it inherently creates a disconnect from the physical constraints of real-world applications. Because these datasets primarily emphasize descriptive reasoning over active, physical interaction, a critical bottleneck emerges: superior semantic comprehension does not invariably translate to proficient task execution in complex, real-world environments. Conversely, alternative lines of research (Qu et al., 2025c; Yuan et al., 2025a; Li et al., 2026; Zheng et al., 2024) attempt to bridge this gap by explicitly integrating spatial, temporal, and low-level physical knowledge directly into downstream VLA models (Kim et al., 2024; Team et al., 2024) to enhance operational performance. However, these low-level physical priors are typically injected late in the pipeline or treated as separate entities from the broad textual pre-training data. This isolates critical physical grounding from the rich, open-vocabulary semantic guidance of linguistic models, preventing the development of a truly unified, embodied representation. Consequently, a critical and emerging question arises: how can we seamlessly embed essential spatial and physical knowledge directly into the foundational pre-training phase of vision-language models, such that it tangibly elevates both abstract semantic reasoning and actionable, real-world operational intelligence?

To overcome these limitations, we propose **GEM**, a **Generative-supervised Embodied** vision-language model. To effectively capture fine-grained structural details and complete spatial and geometric relations within visual scenes, we establish depth map prediction (Lin et al., 2025) as an intrinsic generative target. This is achieved through a novel hybrid autoregressive-diffusion architecture (Chen et al., 2025a; Wu et al., 2025a) designed to seamlessly blend generative and representational supervision. Specifically, our approach conditions a diffusion transformer (Peebles and Xie, 2023; Lipman et al., 2022) on the hidden visual features extracted by an auto-regressive understanding model (Bai et al., 2025) to synthesize accurate depth maps. To facilitate this integration, we implement a progressive training strategy that initially stabilizes the generation module before jointly optimizing for both depth synthesis and linguistic knowledge acquisition. Furthermore,

to synergize with our architectural and training advancements, we introduce GEM-4M, a high-quality, large-scale embodied pre-training dataset. GEM-4M encompasses extensive embodied question-answering pairs that rigorously cover physical grounding, spatial-temporal planning, and physical reasoning tasks. Ultimately, the comprehensive spatial and semantic representations learned by the GEM architecture can be effortlessly extended into a VLA model, denoted as GEM-VLA, facilitating robust, autonomous performance in real-world robotic deployments.

Extensive experimental evaluations demonstrate that GEM and GEM-VLA show remarkable performance under a wide range of benchmarks from recognition to real-world operations. GEM establishes a new state-of-the-art, consistently outperforming leading open-source general-purpose models, as well as spatial and embodied specialists, on key reasoning benchmarks. Specifically, GEM attains the highest overall scores on the challenging spatial-related benchmarks (Yang et al., 2024; 2025f; Du et al., 2024; Tong et al., 2024) and shows large gains over its initialization backbones. For instance, the VSI-Bench (Yang et al., 2024) score improves from 50.4 to 62.8 for the 2B model and from 57.9 to 70.6 for the 8B model. On benchmarks that require fine-grained spatial grounding (Zhou et al., 2025; Yuan et al., 2024; Song et al., 2025a), GEM far exceeds the performance of the strong proprietary baseline, Gemini-3-Pro, by 10%. Furthermore, our vision-language-action model, GEM-VLA, achieves a record-breaking 96.1% average success rate on the LIBERO (Liu et al., 2023a) benchmark, outperforming standard VLAs such as π_0 and spatial-enhanced VLAs (Qu et al., 2025c; Yuan et al., 2025a). GEM-VLA also transfers robustly to challenging real-world settings and surpasses recent methods (Pertsch et al., 2025; Intelligence et al., 2025a) with an average success rate of 43%, marking a substantial improvement over the previous state-of-the-art’s 28.7%.

2 Related Work

2.1 Vision-Language Models for Embodied Intelligence

Enhancing the embodied reasoning capabilities of state-of-the-art Vision-Language Models (VLMs) has become a central research focus. A number of data-driven methodologies have emerged to support such reasoning capabilities, including object affordances for manipulation, object counting, spatial relationship understanding, and action planning that determines subsequent steps based on the current states. For instance, some studies (Team et al., 2025; Azzolini et al., 2025; Luo et al., 2025; Lee et al., 2025a; Qu et al., 2025b; Yang et al., 2025b; Hao et al., 2025b; Qu et al., 2025a) contribute curated datasets specifically tailored for embodied tasks, emphasizing multi-modal understanding and action-aware visual-language alignment. Additionally, other works (Ji et al., 2025; Yuan et al., 2025b; Dang et al., 2026; Zhou et al., 2025; Zhang et al., 2025d) construct synthetic spatiotemporal reasoning datasets enriched with Chain-of-Thought (CoT) annotations (Wei et al., 2022) and then incorporate Reinforcement Fine-Tuning (RFT) (Shao et al., 2024) to further refine reasoning performance of Embodied VLMs. Nevertheless, existing approaches mainly focus on high-level semantic understanding, while overlooking the explicit modeling of fine-grained structural information in visual inputs. As a result, the visual features fail to preserve fine-grained geometric cues, leading to ambiguous spatial relationships. This issue is particularly critical for embodied tasks, where precise perception of object geometry and relative distances is essential for robust manipulation and interaction. In this paper, we imitate this issue by introducing generative supervision to facilitate the fusion of structural and semantic features for more comprehensive embodied reasoning.

2.2 Spatial-Aware Vision-Language-Action Models

Robotic manipulation has evolved from single-task specialists to generalist models trained on broad, diverse datasets. Fueled by advances in VLMs (Beyer et al., 2024; Bai et al., 2025; Wang et al., 2025a; Comanici et al., 2025), and large-scale robot action datasets (Bu et al., 2025; O’Neill et al., 2024; Wu et al., 2024; Khazatsky et al., 2024; Wu et al., 2025b), this evolution has given rise to the architecture of Vision-Language-Action (VLA) models (Brohan et al.,

2022; Kim et al., 2024; Team et al., 2024; Intelligence et al., 2025b; Cheang et al., 2025; Li et al., 2023; Liu et al., 2026; Wen et al., 2025; Liu et al., 2025b), which integrate the VLM backbone with robot action output head. Inheriting the rich perceptual and linguistic representations of pretrained VLMs, VLA models demonstrate improved adaptability and zero-shot capabilities in interpreting and executing human instructions. Despite their promising performance, current VLAs are primarily confined to 2D observation inputs and lack precise perception and comprehension of the 3D physical world. To bridge this gap, early efforts augmented VLAs with 3D or 2.5D inputs (Li et al., 2026; Ze et al., 2024; Zhen et al., 2024; Li et al., 2025b; Zheng et al., 2024). However, such approaches suffer from expensive computational and data acquisition costs. More recent works (Li et al., 2025a; Qu et al., 2025c; Yuan et al., 2025a; Wu et al., 2026; Song et al., 2025b) instead explore various implicit enhancement strategies that integrate global spatial context into the semantic representations from 2D observations, to inject geometric priors. Nevertheless, these methods mainly rely on simple feature fusion, which limits their ability to substantially improve spatial perception. Other works (Zhang et al., 2025c; Zhao et al., 2025a; Zhang et al., 2025b; Jiang et al., 2025; Cen et al., 2025; Wang et al., 2025b; Hu et al., 2024; Liao et al., 2025; Lv et al., 2025) incorporate generative world models that predict future frames or states to inject world knowledge. Although this improves planning by simulating futures, it contributes little to strengthening the geometric encoding of the current scene. Overall, enhancing VLAs with robust and physically grounded perception of the real world remains an open and challenging problem.

3 Method

In this section, we detail our design of GEM’s overall framework. We elaborate our architecture design in Sec. 3.1 and progressive training pipeline in Sec.3.2. Then we describe the construction of our training dataset GEM-4M in Sec.3.3. Finally, we explain how we extend our model to a VLA framework for downstream robot tasks in Sec. 3.4.

3.1 Architecture

In current VLMs, given an instruction l and visual input o , the VLM backbone M_θ encodes them into multimodal token representations $\mathbf{h} = (\mathbf{h}_o, \mathbf{h}_l) = M_\theta(o, l)$ at its final layer. Then they are trained to maximize the likelihood of the target token sequence y , typically using a cross-entropy objective for supervised fine-tuning:

$$\mathcal{L}_{\text{CE}} = - \sum_{i=1}^T \log p_\theta(y_i | y_{<i}, \mathbf{h}_o, \mathbf{h}_l) \quad (1)$$

This objective helps the models align visual token features with text and perform semantic understanding tasks. Despite demonstrating outstanding performance in various visual tasks, their spatial reasoning ability, particularly in embodied scenarios, is limited because \mathbf{h}_o contains only semantic information from o and lacks sufficient physical structural cues for accurate spatial understanding and manipulation in real-world environments.

To address this, we introduce a depth generative objective for supervision. As illustrated in Figure 2, GEM consists of a VLM backbone M_θ , a lightweight connector C_ϕ and a Diffusion Transformer (DiT)-based depth generative head G_ψ . In our design, the visual tokens in \mathbf{h} , denoted as \mathbf{h}_o , are projected into a conditional embedding space via the connector: $\mathbf{c} = C_\phi(\mathbf{h}_o)$. We propose to utilize \mathbf{c} as the condition for the generative head to reconstruct the observation o ’s depth map d . We then employ a flow matching objective $\mathcal{L}_{\text{flow}}$ to optimize the generative head, which learns the vector field v_t at each timestep $t \sim \mathcal{U}(0, 1)$ that transforms a noised distribution \mathbf{x}_t into the ground-truth depth d :

$$\mathcal{L}_{\text{flow}} = \mathbb{E}_{d, t \sim \mathcal{U}(0, 1), \epsilon \sim \mathcal{N}(0, \mathbf{I})} \left[\|\mathbf{v}_t(\mathbf{x}_t, \mathbf{c}) - \mathbf{u}_t(\mathbf{x}_t | d)\|^2 \right] \quad (2)$$

where $\mathbf{u}_t(\mathbf{x}_t | d)$ is the ground-truth velocity field that transforms \mathbf{x}_t into depth d . We combine this generative supervision loss with \mathcal{L}_{CE} to allow \mathbf{h}_o to encode adequate structural information for depth generation, as well as sufficient semantic information for inference.

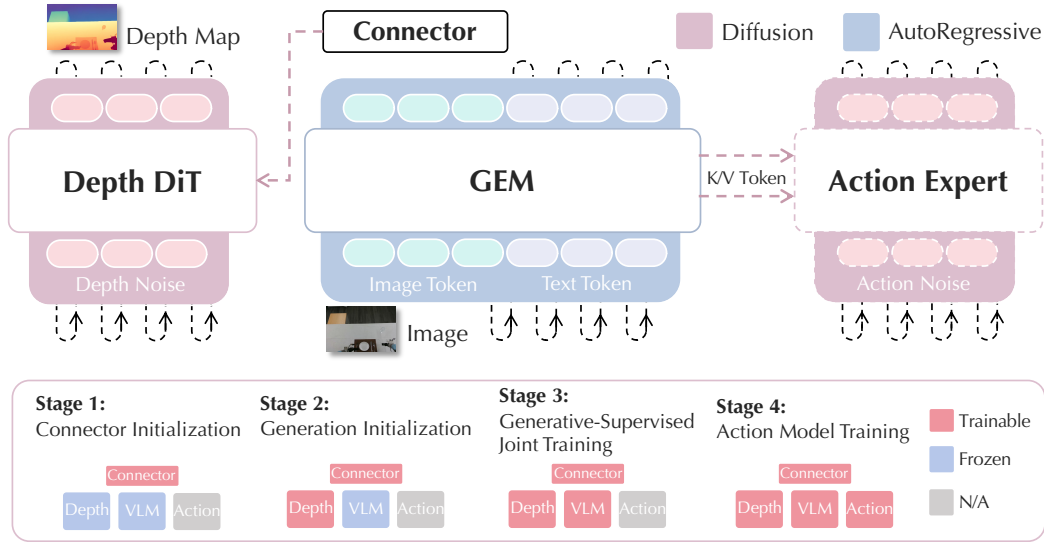


Fig. 2: **Architecture of GEM.** GEM augments a VLM backbone with a DiT-based depth generator conditioned on the backbone’s final-layer visual tokens. We adopt a progressive training paradigm: (i) initialize the connector, (ii) warm up the depth generator, (iii) perform end-to-end joint training, and (iv) train an autoregressive action expert on GEM’s multi-modal tokens. Building on GEM, the GEM-based VLA predicts continuous actions from these representations, improving robot manipulation.

3.2 Progressive Training Recipe

Since there is a gap between the backbone’s output space and the DiT’s input space, directly training the overall framework end-to-end may cause modality interference between the generative head and the VLM backbone, leading to unstable convergence. To address this, we adopt a progressive training recipe to bridge the gap between the two feature spaces effectively. Specifically, the training pipeline is divided into the following three distinct phases:

3.2.1 Stage 1: Connector Initialization

In the first stage, we freeze both the pre-trained VLM backbone and the DiT generative head, and only optimize the connector for preliminary feature alignment. The connector projects the backbone’s semantic representations into the DiT’s input feature space to establish a stable start for later training stages. At this stage, only the generative objective $\mathcal{L}_{\text{flow}}$ is used.

3.2.2 Stage 2: Generative Head Initialization

After preliminary feature alignment, the generative head has not yet adapted to the conditioning features from the VLM backbone. Therefore, we freeze the backbone and only optimize both the connector and DiT head to equip the depth generative head with basic image generation ability. At this stage, the generative objective $\mathcal{L}_{\text{flow}}$ is used solely to transform high-level semantic features into fine-grained structure features, building the foundation for subsequent joint training.

3.2.3 Stage 3: Generative-Supervised Joint Training

In the final stage, we perform end-to-end generative-supervised joint training. Since the first two stages have established a stable initialization, we unfreeze the trainable parameters of the entire framework, including VLM backbone, connector, and DiT head, to foster synergy between the backbone’s semantic understanding and DiT’s generative capability. This allows VLM not only to understand semantics but also to refine its representations to

be more structure-aware, capturing subtle geometric cues and spatial relationships. At this stage, both cross-entropy text loss \mathcal{L}_{CE} and flow-matching generative loss \mathcal{L}_{flow} supervise the training process, with the total loss defined as $\mathcal{L}_{total} = \mathcal{L}_{CE} + \lambda\mathcal{L}_{flow}$, where λ is the balancing weight.

3.3 Dataset

To advance the capability of GEM in perception and reasoning real-world scenarios grounded in physical knowledge, we construct a high-quality, large-scale question-answer (QA) dataset, GEM-4M, for supervised fine-tuning. Here we present an overview of the data building engine and sources, while more details about the construction methodologies are provided in the supplementary materials.

3.3.1 Embodied Grounding Data

To enhance the model’s object recognition and localization capacities in embodied scenarios, we collect 1M high-quality question-answer pairs to support multiple grounding tasks, including open-vocabulary object detection with bounding boxes, localizing objects from instructions, and recognizing object affordances. These data are sourced from several publicly available embodied grounding datasets, such as PACO-LVIS (Ramanathan et al., 2023), RoboPoint (Yuan et al., 2024), RoboAfford (Hao et al., 2025a), ShareRobot (Ji et al., 2025), and Roborefit (Lu et al., 2023). Additionally, to ensure grounding in physical manipulation scenarios, we generate approximately 100k point and bounding box annotations from open-source robot action datasets (Wu et al., 2024; Khazatsky et al., 2024; Bu et al., 2025; O’Neill et al., 2024) using SAM3 (Carion et al., 2025). This combination of open-source and self-curated data covers a wide range of scenarios, enhancing the diversity and generalization of visual grounding in real-world embodied environments. To handle varying image resolutions, both bounding boxes and points are normalized to the range $[0, 1000]$ to ensure consistency.

3.3.2 Physical, Spatial Reasoning Data

This category of data aims to help the model build a foundational understanding of the physical world, such as measurement estimation and spatiotemporal reasoning. Specifically, We incorporate open-source spatial datasets, including MindCube (Yin et al., 2025), ViCA (Feng, 2025), SPAR (Zhang et al., 2025a), and VSI-590K (Yang et al., 2025e), to support 3D spatial reasoning and physical attribute perception. Additionally, we also augment these datasets with 100k manually annotated spatial understanding samples from publicly available 3D scene datasets (Dai et al., 2017; Yeshwanth et al., 2023; Baruch et al., 2021), following the data processing pipeline proposed in VSI-Bench (Yang et al., 2025e). To improve spatiotemporal abilities especially in robot tasks, we integrate 1 million question-answer pairs aggregated from multiple publicly available datasets, such as RoboVQA (Seramanet et al., 2024), Robo2VLM (Chen et al., 2025b), and RefSpatial (Zhou et al., 2025). The integration of these diverse, high-quality data sources strengthens the model’s spatial awareness and boosts performance in complex embodied reasoning tasks.

3.3.3 Spatiotemporal Planning Data

To equip the embodied brain with the ability to plan sub-tasks and forecast the trajectory of each atomic action, we collect data from public robot datasets (Wu et al., 2025b; Bu et al., 2025; Wu et al., 2024) with sub-task annotations and construct question-answer pairs. We extract individual frames from entire egocentric videos based on sub-task annotations and identify the manipulated object in each sub-task description using Qwen3 (Yang et al., 2025a). We then use SAM3 (Carion et al., 2025) to generate object masks and track their trajectory using CoTracker3 (Karaev et al., 2025). Finally, based on the sub-task descriptions and visualized trajectories, we create sub-task and trajectory planning question-answer pairs respectively following the RoboVQA (Seramanet et al., 2024) and MolmoACT (Lee et al., 2025a) templates, resulting in a dataset of approximately 50K samples. The integration

Table 1: **Performance on embodied reasoning benchmarks for spatial understanding across different model types.** The highest and second-highest accuracy values are highlighted in **bold** and underlined, respectively. GEM-8B achieves state-of-the-art (SOTA) performance and near-SOTA competitive results across general-purpose and spatial specialist models.

Models	CV-Bench	VSI-Bench		MMSI-Bench	EmbSpatial	
	All \uparrow	Abs. Dist.	Rel. Dist.	All \uparrow	All \uparrow	
Gemini-3-Pro (Comanici et al., 2025)	82.5	42.8	56.6	53.0	45.9	81.0
Seed1.8 (Seed)	86.5	28.0	50.3	47.2	34.6	78.7
GPT-4o (Hurst et al., 2024)	78.6	5.3	37.0	34.0	30.3	71.9
Qwen3-VL-2B (Bai et al., 2025)	80.0	40.7	49.6	50.4	23.6	69.0
Qwen3-VL-8B (Bai et al., 2025)	85.1	47.5	58.2	57.9	27.7	77.7
InternVL3.5-8B (Wang et al., 2025a)	81.5	40.9	47.7	54.1	28.4	74.2
LLava-OneVision-7B (Li et al., 2024a)	61.9	20.2	42.5	32.4	26.6	73.1
SpaceR-7B (Ouyang et al., 2025)	74.8	28.6	38.2	35.8	26.4	65.8
VLM-3R (Fan et al., 2025)	71.8	49.4	65.4	60.7	27.9	68.2
VST-7B (Yang et al., 2025d)	83.5	43.8	60.0	60.6	32.6	73.6
CambrainS-7B (Yang et al., 2025e)	76.9	49.4	66.9	67.5	24.2	70.0
SenseNova-SI-8B (Cai et al., 2025)	83.2	48.0	64.1	67.9	43.3	77.6
Qwen3-VL-2B-SFT	80.7	45.1	62.2	60.0	28.9	72.7
GEM-2B (Ours)	81.4	48.4	64.1	62.8	30.6	73.0
Qwen3-VL-8B-SFT	<u>85.6</u>	<u>53.7</u>	<u>71.4</u>	<u>68.6</u>	32.8	<u>78.3</u>
GEM-8B (Ours)	86.6	56.3	72.3	70.6	<u>35.3</u>	79.4

of these spatiotemporal data allows the model to combine basic skills, generalize to new scenarios, and plan actions effectively.

3.4 Expanding to Vision-Language Action Model

We integrate GEM into a VLA framework to evaluate its transfer to robotic manipulation. As illustrated in Figure 2, we integrate a Diffusion Transformer (DiT)-based action expert, denoted as A_ω , to generate continuous actions from multi-modal observations via a diffusion policy. We extract the key-value tokens of the multimodal observation history \mathcal{O} from the attention blocks in backbone M_θ and use it as the conditioning representation \mathbf{c}_{act} for the action expert A_ω , to bridge high-level reasoning capabilities and low-level action generation. We perform end-to-end joint optimization of the VLM M_θ , the depth generative head G_ψ , and the action expert A_ω using a combination of both depth and action generative objectives. Specifically, the action objective $\mathcal{L}_{\text{action}}$ aims to predict the vector field \mathbf{v}_t at each timestep $t \sim \mathcal{U}(0, 1)$ that transforms a noisy action state $\mathbf{a}_t = (1 - t)\epsilon + t\mathbf{a}$ into the ground-truth action chunk \mathbf{a} :

$$\mathcal{L}_{\text{action}} = \mathbb{E}_{\mathcal{O}, \mathbf{a}, \epsilon \sim \mathcal{N}(\mathbf{0}, \mathbf{I}), t \sim \mathcal{U}(0, 1)} \left[\|\mathbf{v}_t(\mathbf{a}_t, \mathbf{c}_{\text{act}}) - \mathbf{u}_t(\mathbf{a}_t | \mathbf{a})\|_2^2 \right] \quad (3)$$

The total loss is then defined as: $\mathcal{L}_{\text{total}} = \mathcal{L}_{\text{action}} + \lambda \mathcal{L}_{\text{flow}}$, where λ is the same balancing weight.

4 Experiments

4.1 Implementation Details

We adopt Qwen3-VL (Bai et al., 2025) as our VLM backbone and Sana (Xie et al., 2024) as the depth prediction head. We define a light connector comprising 2 layers of MLP that bridge the backbone’s output space with the DiT’s input space. Since some of our training data lack ground-truth depth annotations, we use DepthAnythingv3 (Lin et al., 2025) to generate pseudo depth maps for supervision. We train for 500 steps in Stage 1, 4k steps in Stage 2, and 1 epoch in Stage 3. We set $\lambda = 0.1$ to balance structural synthesis with semantic understanding. The training process is performed on 32 NVIDIA A800 GPUs,

Table 2: Performance on the object placement and grounding spatial benchmarks across different model types. The highest and second-highest accuracy values are highlighted in bold and underlined. * denotes results obtained from their reports. It shows that GEM-8B achieves the best performance, compared with general-purpose and embodied specialist models.

Models	RefSpatial			Where2Place		RoboSpatial	
	Loc.	Pla.	All ↑	Seen	Unseen	All ↑	All ↑
Gemini-3-Pro (Comanici et al., 2025)	30.0	35.0	34.3	58.6	43.3	54.0	57.4
Seed1.8 (Seed)	65.0	41.0	50.2	54.2	53.3	53.8	66.9
GPT-4o (Hurst et al., 2024)	8.00	9.55	8.78	20.3	20.7	20.4	43.5
Qwen3-VL-2B (Bai et al., 2025)	36.0	29.0	27.4	45.7	43.3	45.0	40.7
Qwen3-VL-8B (Bai et al., 2025)	<u>54.0</u>	36.7	38.0	61.0	62.2	61.3	65.4
VeBrain-8B(Luo et al., 2025)	0.03	0.57	0.30	12.3	9.17	11.3	42.5
Magma-8B (Yang et al., 2025c)	1.00	8.00	4.50	9.93	13.1	10.9	33.7
RoboBrain-2.0-7B* (Ji et al., 2025)	36.0	29.0	32.5	<u>64.3</u>	61.9	<u>63.6</u>	54.2
Mimo-Embodied-7B* (Hao et al., 2025b)	-	-	48.0	-	-	<u>63.6</u>	61.8
Cosmos-Reason2-8B (Azzolini et al., 2025)	48.0	27.0	33.2	52.9	43.3	50.0	<u>65.7</u>
Qwen3-VL-2B-SFT	37.0	29.0	29.6	56.7	51.4	53.0	44.6
GEM-2B (Ours)	41.0	33.0	32.1	52.8	53.3	53.0	47.4
Qwen3-VL-8B-SFT	53.0	40.0	<u>45.8</u>	60.0	<u>62.9</u>	62.0	65.4
GEM-8B (Ours)	57.0	<u>38.0</u>	44.4	65.7	63.3	65.0	66.9

with a cosine learning rate scheduler from $1e - 5$ to $1e - 6$. In real-world VLA tasks, we adopt the dedicated action expert from RDT2 (Liu et al., 2026). For each specific task, we jointly fine-tune the entire framework for 50k steps on 8 NVIDIA A800 GPUs, with a linear scheduler and a learning rate of $1e - 5$. The balancing weight λ in VLA finetuning is also set to 0.1. More implementation details can be seen in the supplementary material.

4.2 Evaluation on Embodied Reasoning Capacities

We evaluate on public spatiotemporal embodied reasoning benchmarks, including CV-Bench (Tong et al., 2024), VSI-Bench (Yang et al., 2024), MMSI-Bench (Yang et al., 2025f) and EmbSpatial (Du et al., 2024). As shown in Table 1, both scales of GEM yield significant improvements across all tasks compared to their base models, Qwen3-VL. For instance, on the challenging VSI-Bench and MMSI-Bench, GEM improves the scores by roughly 10%. In particular, compared with open-source general-purpose baselines (Bai et al., 2025; Wang et al., 2025a; Li et al., 2024a), the 8B-scale variant of GEM achieves the strongest overall performance on the majority of benchmarks, and remains highly competitive on the remaining. Furthermore, it also achieves superior performance even when compared to spatial specialist models (Fan et al., 2025; Ouyang et al., 2025; Yang et al., 2025d; Cai et al., 2025). These strong results highlight our model’s powerful spatiotemporal reasoning capabilities, which can be effectively transferred to downstream tasks.

We further evaluate our model on benchmarks, including RefSpatial (Zhou et al., 2025), Where2Place (Yuan et al., 2024), and RoboSpatial (Song et al., 2025a), which focus on object placement and referring in embodied environments. The results summarized in Table 2 show that the 8B variant of GEM achieves the best overall performance compared with both general-purpose and embodied specialist models (Luo et al., 2025; Yang et al., 2025c; Ji et al., 2025; Hao et al., 2025b; Azzolini et al., 2025), while the 2B variant also remains highly competitive with many larger-scale models (Azzolini et al., 2025; Yang et al., 2025c; Luo et al., 2025). It is also worth noting that GEM exceeds the strong proprietary baseline, Gemini-3-Pro (Team et al., 2025), by about 10% on average across benchmarks. Such competence highlights GEM’s outstanding spatial reasoning capabilities in embodied environments, making it a versatile backbone for embodied AI brains.

Moreover, to assess the impact of depth generative supervision, we exclude this component and fine-tune the base models on the constructed dataset, referred to as Qwen3VL-2B-SFT and Qwen3VL-8B-SFT. As shown in Table 1 and Table 2, the performance of both scales

Table 3: **Success rates on the LIBERO benchmark across four task suites.** It is demonstrated that GEM-VLA exhibits better performance than all baselines, suggesting that implicit geometry reasoning from depth generative supervision improves generalization across diverse manipulation tasks.

Models	Spatial	Object	Goal	Long	Average \uparrow
Diffusion Policy (Chi et al., 2025)	78.3	92.5	68.3	50.5	72.4
Octo-Base (Team et al., 2024)	78.9	85.7	84.6	51.1	75.1
OpenVLA (Kim et al., 2024)	84.7	88.4	79.2	53.7	76.5
π_0 (reported) (Intelligence et al., 2025b)	96.8	98.8	95.8	85.2	94.2
TraceVLA (Zheng et al., 2024)	84.6	85.2	75.1	54.1	74.8
SpatialVLA (Qu et al., 2025c)	88.2	89.9	78.6	55.5	78.1
MolmoACT (Lee et al., 2025b)	87.0	95.4	87.6	77.2	86.6
DreamVLA (Zhang et al., 2025c)	97.5	94.0	89.5	59.5	92.6
DepthVLA (Yuan et al., 2025a)	96.4	98.0	95.8	89.2	94.9
Qwen3VL-SFT-VLA	97.2	98.4	95.6	88.4	94.9
GEM-VLA (Ours)	99.0	98.8	97.1	89.3	96.1

drops compared to the full models. This is because the full model leverages generative supervision to integrate global structural features with semantic features within a shared representation space, which benefits stronger spatial perception capabilities. Notably, on distance-related questions in VSI-Bench (Yang et al., 2024), the full models significantly outperform their counterparts, demonstrating that depth supervision enhances the model’s ability to perceive relative distance and spatial relationships.

4.3 Evaluation on Downstream VLA tasks

4.3.1 Simulation Evaluation

We perform evaluation on the widely adopted LIBERO benchmark (Liu et al., 2023a). It comprises four task suites: Spatial, Object, Goal, and Long, each containing 10 diverse tasks with 50 trials per task. For comprehensive comparison, we select high-performance VLA models, including both standard models (Chi et al., 2025; Kim et al., 2024; Intelligence et al., 2025b; Team et al., 2024) and spatially-enhanced VLA models (Zheng et al., 2024; Qu et al., 2025c; Zhang et al., 2025c; Lee et al., 2025b; Yuan et al., 2025a) as baselines. Unlike prior models pre-trained on robot data, we fine-tune GEM-2B and its action expert from scratch for action prediction on LIBERO for 20k steps, following the StarVLA implementation (starVLA Contributors, 2025). The evaluation results, shown in Table 3, demonstrate that GEM-VLA achieves the highest success rate across all task types. This indicates that despite large-scale action pretraining, standard VLAs still lack sufficient spatial grounding for precise manipulation. Furthermore, GEM-VLA also outperforms other spatially enhanced VLAs, showcasing the strongest physical grounding capacities. Additionally, the performance of the VLA based on GEM also surpasses that based on the standard SFT model, which further underscores the benefit of depth generative supervision for accurate action prediction.

4.3.2 Real-World Evaluation

We extend GEM to GEM-VLA following the approach in Sec. 3.4, and deploy it on a UR5 platform to evaluate its performance on real-world manipulation tasks. We compare our model with most advanced baselines π_0 -FAST (Pertsch et al., 2025) and $\pi_{0.5}$ (Intelligence et al., 2025a). We finetune each model on several challenging real-world tasks, including long-horizon tasks (e.g., table bussing) and deformable object manipulation (e.g., folding clothes, unzipping a zipper). Task descriptions are shown in Figure 4.

As summarized in Figure 3, our GEM-VLA demonstrates superior performance across all task and subtask categories. In both deformable manipulation tasks, GEM achieves higher success rates than all baselines (Intelligence et al., 2025a; Pertsch et al., 2025), particularly on the complex multi-step cloth folding task. For the long-horizon table bussing task, GEM-VLA achieves a significantly higher average progress score, which indicates its stronger

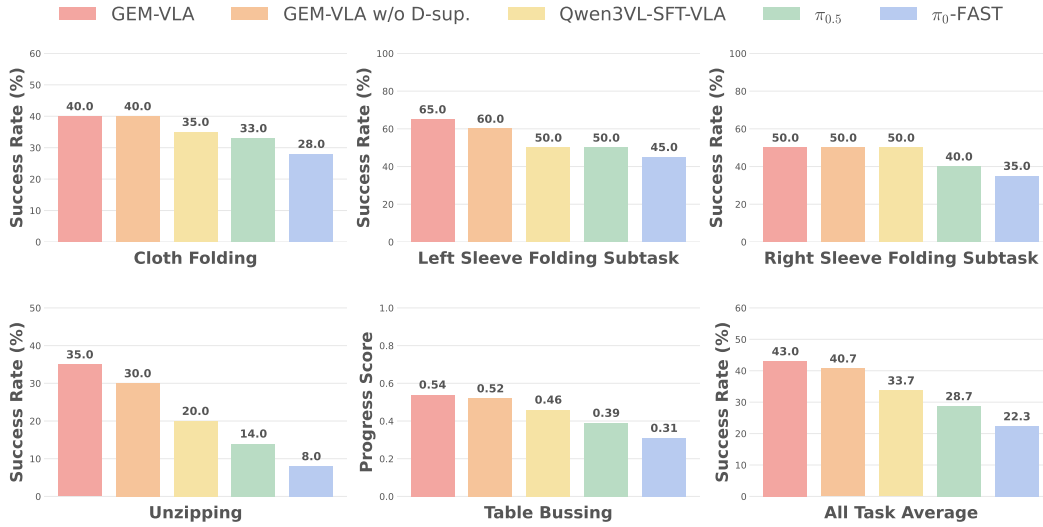


Fig. 3: Comparison of GEM and baseline models on challenging real-world tasks. The progress score refers to the average percentage of sub-tasks completed in the long-horizon task. It is noted that the full GEM-VLA model outperforms previous baselines in success rate and progress score across all tasks and sub-tasks.

long-horizon robustness and stability. These results confirm that GEM effectively transfers its pre-trained physical knowledge to state-of-the-art performance in diverse challenging real-world robotic manipulation.

Moreover, we also investigate the effectiveness of depth generative supervision during VLA fine-tuning. We freeze the depth head and train only the VLM backbone and action expert with the action objective in Eq. 3. As shown in the Figure 3, performance drops on almost all tasks when depth generative supervision is removed, indicating that auxiliary depth prediction enables more accurate manipulation. Notably, the VLA fine-tuned from pre-trained GEM still outperforms its counterpart finetuned on the standard SFT model, which suggests that depth generative supervision facilitates learning physical priors in the embodied VLM, translating into stronger performance on downstream robot tasks.

5 Ablation Studies

5.1 Superiority of Depth Supervision over RGB

We investigate why depth is a more suitable supervisory signal compared to other alternatives. Specifically, we compare our depth-based generation with an RGB-based image generation task, where the model is trained to regenerate the input image. For fair comparison, we fine-tune both models on the open-source VSI-590K dataset (Yang et al., 2025e), keeping all other training hyper-parameters and strategies default. We evaluate each model on the representative spatial reasoning benchmarks, including CV-Bench (Tong et al., 2024), VSI-Bench (Yang et al., 2024), and RoboSpatial (Song et al., 2025a).

The results, summarized in Table 4 (rows 1 and 3), reveal that replacing depth supervision with RGB reconstruction leads to inferior performance, particularly on distance-related questions in VSI-Bench. This suggests depth provides more explicit cues about spatial relationships, such as relative distance, making it a more effective supervisory signal than RGB.

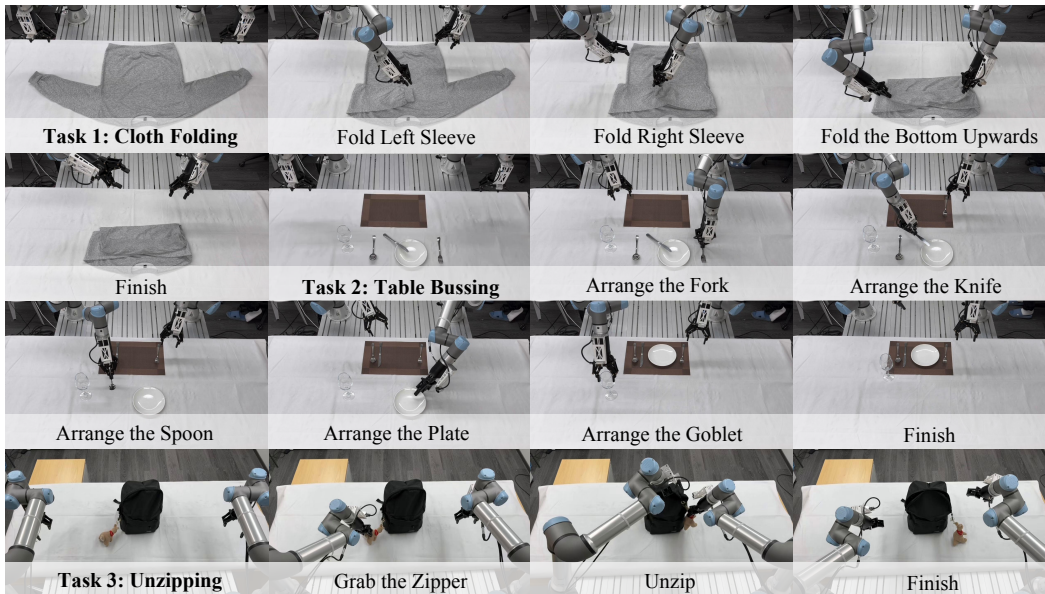


Fig. 4: Demonstrations of three finetuned real-robot tasks, including one long-horizon task **table bussing** and two deformable object manipulation tasks **folding clothes** and **unzipping a backpack’s zipper**.

Table 4: **Comparison between GEM and different settings.** The results show that the default model yields the best performance, which indicates depth supervision enhances structural learning compared to RGB and direct end-to-end training fails to effectively integrate semantic and structural features.

Models	CV-Bench	VSI-Bench		RoboSpatial	
	All \uparrow	Abs. Dist.	Rel. Dist.	All \uparrow	All \uparrow
RGB Supervision	80.9	47.5	62.8	60.0	44.6
Direct End-to-End Co-Training	79.7	42.1	60.0	57.6	44.0
Default Setting (GEM)	81.1	47.8	65.2	63.0	48.9

5.2 Effectiveness of Progressive Training Strategy

We evaluate the effectiveness of the proposed progressive three-stage training strategy. To compare, we perform a direct end-to-end training on both the depth generative head and understanding backbone using the VSI-590K dataset (Yang et al., 2025e), and evaluate its performance on the same benchmarks (Tong et al., 2024; Yang et al., 2024; Song et al., 2025a) above. The comparison results are shown in Table 4, in the second and third rows. It can be observed that direct end-to-end training underperforms the default three-stage training paradigm. This is because the generative head and connector fail to receive an appropriate initialization, which limits the effective fusion of semantic and structural features. Therefore, direct end-to-end co-training negatively affects the understanding model’s performance.

5.3 Effect of Generative Supervision on Structural Priors Learning

To assess whether depth generative supervision improves structural awareness in GEM, we respectively feed the final-layer visual token features from both Qwen3-VL-SFT and GEM into depth generator. As illustrated in Figure 5, the generated results of Qwen3-VL-SFT exhibit limited structural details. This indicates that visual representations learned under standard SFT are dominated by high-level semantic signals, while explicit spatial and geometric information is limited. This also accounts for the suboptimal embodied

reasoning performance in standard SFT models. In contrast, GEM presents high-fidelity depth generation results, highlighting the effectiveness of depth generative supervision in capturing crucial low-level structural information from 2D inputs.



Fig. 5: **Comparison of generation results from visual features in GEM and Qwen3-VL-SFT.** The results generated using only semantic features from the standard SFT model exhibit limited structural details, while GEM features produce high-quality results. This is because generative supervision helps the model capture structural cues that are beneficial for spatial perception in embodied environments.

6 Conclusion

In this paper, we introduce GEM, a novel Generative-supervised Embodied vision-language framework designed to bridge the gap between high-level semantic reasoning and low-level physical grounding by learning depth generation as an intrinsic target for scene geometry. A progressive training recipe is adopted to optimize depth synthesis and language objectives to better fuse structural and semantic representations. Beyond architectural and training advancements, we also construct a large-scale dataset that covers various embodied tasks to support training. Extensive evaluations demonstrate that GEM achieves strong performance across a variety of embodied benchmarks. Furthermore, the VLA model built on GEM sets new records on simulation benchmarks and shows robust generalization in real-world robotic tasks.

References

- Alisson Azzolini, Junjie Bai, Hannah Brandon, Jiaxin Cao, Prithvijit Chattopadhyay, Huayu Chen, Jinju Chu, Yin Cui, Jenna Diamond, Yifan Ding, et al. Cosmos-reason1: From physical common sense to embodied reasoning. *arXiv preprint arXiv:2503.15558*, 2025.
- Shuai Bai, Yuxuan Cai, Ruizhe Chen, Keqin Chen, Xionghui Chen, Zesen Cheng, Lianghao Deng, Wei Ding, Chang Gao, Chunjiang Ge, et al. Qwen3-vl technical report. *arXiv preprint arXiv:2511.21631*, 2025.
- Gilad Baruch, Zhuoyuan Chen, Afshin Dehghan, Tal Dimry, Yuri Feigin, Peter Fu, Thomas Gebauer, Brandon Joffe, Daniel Kurz, Arik Schwartz, et al. Arkitscenes: A diverse real-world dataset for 3d indoor scene understanding using mobile rgb-d data. *arXiv preprint arXiv:2111.08897*, 2021.
- Lucas Beyer, Andreas Steiner, André Susano Pinto, Alexander Kolesnikov, Xiao Wang, Daniel Salz, Maxim Neumann, Ibrahim Alabdulmohsin, Michael Tschannen, Emanuele Bugliarello, et al. Paligemma: A versatile 3b vlm for transfer. *arXiv preprint arXiv:2407.07726*, 2024.
- Anthony Brohan, Noah Brown, Justice Carbajal, Yevgen Chebotar, Joseph Dabis, Chelsea Finn, Keerthana Gopalakrishnan, Karol Hausman, Alex Herzog, Jasmine Hsu, et al. Rt-1: Robotics transformer for real-world control at scale. *arXiv preprint arXiv:2212.06817*, 2022.
- Qingwen Bu, Jisong Cai, Li Chen, Xiuqi Cui, Yan Ding, Siyuan Feng, Xindong He, Xu Huang, et al. Agibot world colosseum: A large-scale manipulation platform for scalable and intelligent embodied systems. In *2025 IEEE/RSJ International Conference on Intelligent Robots and Systems (IROS)*. IEEE, 2025.
- Zhongang Cai, Ruisi Wang, Chenyang Gu, Fanyi Pu, Junxiang Xu, Yubo Wang, Wanqi Yin, Zhitao Yang, Chen Wei, Qingping Sun, Tongxi Zhou, Jiaqi Li, Hui En Pang, Oscar Qian, Yukun Wei, Zhiqian Lin, Xuanke Shi, Kewang Deng, Xiaoyang Han, Zukai Chen, Xiangyu Fan, Hanming Deng, Lewei Lu, Liang Pan, Bo Li, Ziwei Liu, Quan Wang, Dahua Lin, and Lei Yang. Scaling spatial intelligence with multimodal foundation models. *arXiv preprint arXiv:2511.13719*, 2025.
- Nicolas Carion, Laura Gustafson, Yuan-Ting Hu, Shoubhik Debnath, Ronghang Hu, Didac Suris, Chaitanya Ryali, Kalyan Vasudev Alwala, Haitham Khedr, Andrew Huang, Jie Lei, Tengyu Ma, Baishan Guo, Arpit Kalla, Markus Marks, Joseph Greer, Meng Wang, Peize Sun, Roman Rädle, Triantafyllos Afouras, Effrosyni Mavroudi, Katherine Xu, Tsung-Han Wu, Yu Zhou, Liliane Momeni, Rishi Hazra, Shuangrui Ding, Sagar Vaze, Francois Porcher, Feng Li, Siyuan Li, Aishwarya Kamath, Ho Kei Cheng, Piotr Dollár, Nikhila Ravi, Kate Saenko, Pengchuan Zhang, and Christoph Feichtenhofer. Sam 3: Segment anything with concepts, 2025. URL <https://arxiv.org/abs/2511.16719>.
- Jun Cen, Chaohui Yu, Hangjie Yuan, Yuming Jiang, Siteng Huang, Jiayan Guo, Xin Li, Yibing Song, Hao Luo, Fan Wang, et al. Worldvla: Towards autoregressive action world model. *arXiv preprint arXiv:2506.21539*, 2025.
- Chilam Cheang, Sijin Chen, Zhongren Cui, Yingdong Hu, Liqun Huang, Tao Kong, Hang Li, Yifeng Li, Yuxiao Liu, Xiao Ma, et al. Gr-3 technical report. *arXiv preprint arXiv:2507.15493*, 2025.
- Jiuhai Chen, Le Xue, Zhiyang Xu, Xichen Pan, Shusheng Yang, Can Qin, An Yan, Honglu Zhou, Zeyuan Chen, Lifu Huang, et al. Blip3o-next: Next frontier of native image generation. *arXiv preprint arXiv:2510.15857*, 2025a.
- Kaiyuan Chen, Shuangyu Xie, Zehan Ma, Pannag R Sanketi, and Ken Goldberg. Robo2vlm: Visual question answering from large-scale in-the-wild robot manipulation datasets. *arXiv preprint arXiv:2505.15517*, 2025b.
- Cheng Chi, Zhenjia Xu, Siyuan Feng, Eric Cousineau, Yilun Du, Benjamin Burchfiel, Russ Tedrake, and Shuran Song. Diffusion policy: Visuomotor policy learning via action diffusion. *The International Journal of Robotics Research*, 44(10-11):1684–1704, 2025.
- Gheorghe Comanici, Eric Bieber, Mike Schaeckermann, Ice Pasupat, Noveen Sachdeva, Inderjit Dhillon, Marcel Blistein, Ori Ram, Dan Zhang, Evan Rosen, et al. Gemini 2.5: Pushing the frontier with advanced reasoning, multimodality, long context, and next generation agentic capabilities. *arXiv preprint arXiv:2507.06261*, 2025.
- Angela Dai, Angel X Chang, Manolis Savva, Maciej Halber, Thomas Funkhouser, and Matthias Nießner. Scannet: Richly-annotated 3d reconstructions of indoor scenes. In *Proceedings of the IEEE conference on computer vision and pattern recognition*, pages 5828–5839, 2017.

- Ronghao Dang, Jiayan Guo, Bohan Hou, Sicong Leng, Kehan Li, Xin Li, Jiangpin Liu, Yunxuan Mao, Zhikai Wang, Yuqian Yuan, et al. Rynnbrain: Open embodied foundation models. *arXiv preprint arXiv:2602.14979*, 2026.
- Mengfei Du, Binhao Wu, Zejun Li, Xuan-Jing Huang, and Zhongyu Wei. Embspatial-bench: Benchmarking spatial understanding for embodied tasks with large vision-language models. In *Proceedings of the 62nd Annual Meeting of the Association for Computational Linguistics (Volume 2: Short Papers)*, pages 346–355, 2024.
- Zhiwen Fan, Jian Zhang, Renjie Li, Junge Zhang, Runjin Chen, Hezhen Hu, Kevin Wang, Huaizhi Qu, Dilin Wang, Zhicheng Yan, et al. Vlm-3r: Vision-language models augmented with instruction-aligned 3d reconstruction. *arXiv preprint arXiv:2505.20279*, 2025.
- Qi Feng. Visuospatial cognitive assistant. *arXiv preprint arXiv:2505.12312*, 2025.
- Xiaoshuai Hao, Yingbo Tang, Lingfeng Zhang, Yanbiao Ma, Yunfeng Diao, Ziyu Jia, Wenbo Ding, Hangjun Ye, and Long Chen. Roboafford++: A generative ai-enhanced dataset for multimodal affordance learning in robotic manipulation and navigation. *arXiv preprint arXiv:2511.12436*, 2025a.
- Xiaoshuai Hao, Lei Zhou, Zhijian Huang, Zhiwen Hou, Yingbo Tang, Lingfeng Zhang, Guang Li, Zheng Lu, Shuhuai Ren, Xianhui Meng, et al. Mimo-embodied: X-embodied foundation model technical report. *arXiv preprint arXiv:2511.16518*, 2025b.
- Yucheng Hu, Yanjiang Guo, Pengchao Wang, Xiaoyu Chen, Yen-Jen Wang, Jianke Zhang, Koushil Sreenath, Chaochao Lu, and Jianyu Chen. Video prediction policy: A generalist robot policy with predictive visual representations. *arXiv preprint arXiv:2412.14803*, 2024.
- Chi-Pin Huang, Yueh-Hua Wu, Min-Hung Chen, Yu-Chiang Frank Wang, and Fu-En Yang. Thinkact: Vision-language-action reasoning via reinforced visual latent planning. *arXiv preprint arXiv:2507.16815*, 2025.
- Aaron Hurst, Adam Lerer, Adam P Goucher, Adam Perelman, Aditya Ramesh, Aidan Clark, AJ Ostrow, Akila Welihinda, Alan Hayes, Alec Radford, et al. Gpt-4o system card. *arXiv preprint arXiv:2410.21276*, 2024.
- Physical Intelligence, Kevin Black, Noah Brown, James Darpinian, Karan Dhabalia, Danny Driess, Adnan Esmail, Michael Equi, Chelsea Finn, Niccolo Fusai, et al. $\pi_{0.5}$: a vision-language-action model with open-world generalization. *arXiv preprint arXiv:2504.16054*, 2025a.
- Physical Intelligence, Kevin Black, Noah Brown, James Darpinian, Karan Dhabalia, Danny Driess, Adnan Esmail, Michael Equi, Chelsea Finn, Niccolo Fusai, et al. π_0 : a vision-language-action model with open-world generalization. *arXiv preprint arXiv:2504.16054*, 2025b.
- Yuheng Ji, Huajie Tan, Jiayu Shi, Xiaoshuai Hao, Yuan Zhang, Hengyuan Zhang, Pengwei Wang, Mengdi Zhao, Yao Mu, Pengju An, et al. Robobrain: A unified brain model for robotic manipulation from abstract to concrete. *arXiv preprint arXiv:2502.21257*, 2025.
- Yuming Jiang, Siteng Huang, Shengke Xue, Yaxi Zhao, Jun Cen, Sicong Leng, Kehan Li, Jiayan Guo, Kexiang Wang, Mingxiu Chen, et al. Rynnvla-001: Using human demonstrations to improve robot manipulation. *arXiv preprint arXiv:2509.15212*, 2025.
- Nikita Karaev, Yuri Makarov, Jianyuan Wang, Natalia Neverova, Andrea Vedaldi, and Christian Rupprecht. Cotracker3: Simpler and better point tracking by pseudo-labelling real videos. In *Proceedings of the IEEE/CVF International Conference on Computer Vision*, pages 6013–6022, 2025.
- Alexander Khazatsky, Karl Pertsch, Suraj Nair, Ashwin Balakrishna, Sudeep Dasari, Siddharth Karamcheti, Soroush Nasiriany, Mohan Kumar Srirama, Lawrence Yunliang Chen, Kirsty Ellis, et al. Droid: A large-scale in-the-wild robot manipulation dataset. *arXiv preprint arXiv:2403.12945*, 2024.
- Moo Jin Kim, Karl Pertsch, Siddharth Karamcheti, Ted Xiao, Ashwin Balakrishna, Suraj Nair, Rafael Rafailov, Ethan Foster, Grace Lam, Pannag Sanketi, et al. Openvla: An open-source vision-language-action model. *arXiv preprint arXiv:2406.09246*, 2024.
- Jason Lee, Jiafei Duan, Haoquan Fang, Yuquan Deng, Shuo Liu, Boyang Li, Bohan Fang, Jieyu Zhang, Yi Ru Wang, Sangho Lee, Winson Han, Wilbert Pumacay, Angelica Wu, Rose Hendrix, Karen Farley, Eli VanderBilt, Ali Farhadi, Dieter Fox, and Ranjay Krishna. Molmoact: Action reasoning models that can reason in space, 2025a. URL <https://arxiv.org/abs/2508.07917>.
- Jason Lee, Jiafei Duan, Haoquan Fang, Yuquan Deng, Shuo Liu, Boyang Li, Bohan Fang, Jieyu Zhang, Yi Ru Wang, Sangho Lee, et al. Molmoact: Action reasoning models that can reason in space. *arXiv preprint arXiv:2508.07917*, 2025b.

- Bo Li, Yuanhan Zhang, Dong Guo, Renrui Zhang, Feng Li, Hao Zhang, Kaichen Zhang, Peiyuan Zhang, Yanwei Li, Ziwei Liu, et al. Llava-onevision: Easy visual task transfer. *arXiv preprint arXiv:2408.03326*, 2024a.
- Chengmeng Li, Junjie Wen, Yaxin Peng, Yan Peng, and Yichen Zhu. Pointvla: Injecting the 3d world into vision-language-action models. *IEEE Robotics and Automation Letters*, 11(3): 2506–2513, 2026.
- Fuhao Li, Wenxuan Song, Han Zhao, Jingbo Wang, Pengxiang Ding, Donglin Wang, Long Zeng, and Haoang Li. Spatial forcing: Implicit spatial representation alignment for vision-language-action model. *arXiv preprint arXiv:2510.12276*, 2025a.
- Xiaoqi Li, Liang Heng, Jiaming Liu, Yan Shen, Chenyang Gu, Zhuoyang Liu, Hao Chen, Nuowei Han, Renrui Zhang, Hao Tang, et al. 3ds-vla: A 3d spatial-aware vision language action model for robust multi-task manipulation. In *9th Annual Conference on Robot Learning*, 2025b.
- Xinghang Li, Minghuan Liu, Hanbo Zhang, Cunjun Yu, Jie Xu, Hongtao Wu, Chilam Cheang, Ya Jing, Weinan Zhang, Huaping Liu, et al. Vision-language foundation models as effective robot imitators. *arXiv preprint arXiv:2311.01378*, 2023.
- Xuanlin Li, Kyle Hsu, Jiayuan Gu, Karl Pertsch, Oier Mees, Homer Rich Walke, Chuyuan Fu, Ishikaa Lunawat, Isabel Sieh, Sean Kirmani, et al. Evaluating real-world robot manipulation policies in simulation. *arXiv preprint arXiv:2405.05941*, 2024b.
- Yue Liao, Pengfei Zhou, Siyuan Huang, Donglin Yang, Shengcong Chen, Yuxin Jiang, Yue Hu, Jingbin Cai, Si Liu, Jianlan Luo, et al. Genie envisioner: A unified world foundation platform for robotic manipulation. *arXiv preprint arXiv:2508.05635*, 2025.
- Haotong Lin, Sili Chen, Junhao Liew, Donny Y Chen, Zhenyu Li, Guang Shi, Jiashi Feng, and Bingyi Kang. Depth anything 3: Recovering the visual space from any views. *arXiv preprint arXiv:2511.10647*, 2025.
- Yaron Lipman, Ricky TQ Chen, Heli Ben-Hamu, Maximilian Nickel, and Matt Le. Flow matching for generative modeling. *arXiv preprint arXiv:2210.02747*, 2022.
- Bo Liu, Yifeng Zhu, Chongkai Gao, Yihao Feng, Qiang Liu, Yuke Zhu, and Peter Stone. Libero: Benchmarking knowledge transfer for lifelong robot learning. *Advances in Neural Information Processing Systems*, 36:44776–44791, 2023a.
- Haotian Liu, Chunyuan Li, Qingyang Wu, and Yong Jae Lee. Visual instruction tuning. *Advances in neural information processing systems*, 36:34892–34916, 2023b.
- Huaping Liu, Xinghang Li, Peiyan Li, Minghuan Liu, Dong Wang, Jirong Liu, Bingyi Kang, Xiao Ma, Tao Kong, and Hanbo Zhang. Towards generalist robot policies: What matters in building vision-language-action models. 2025a.
- Jiaming Liu, Hao Chen, Pengju An, Zhuoyang Liu, Renrui Zhang, Chenyang Gu, Xiaoqi Li, Ziyu Guo, Sixiang Chen, Mengzhen Liu, et al. Hybridvla: Collaborative diffusion and autoregression in a unified vision-language-action model. *arXiv preprint arXiv:2503.10631*, 2025b.
- Songming Liu, Bangguo Li, Kai Ma, Lingxuan Wu, Hengkai Tan, Xiao Ouyang, Hang Su, and Jun Zhu. Rdt2: Exploring the scaling limit of umi data towards zero-shot cross-embodiment generalization. *arXiv preprint arXiv:2602.03310*, 2026.
- Yuhao Lu, Yixuan Fan, Beixing Deng, Fangfu Liu, Yali Li, and Shengjin Wang. VI-grasp: a 6-dof interactive grasp policy for language-oriented objects in cluttered indoor scenes. In *2023 IEEE/RSJ International Conference on Intelligent Robots and Systems (IROS)*, pages 976–983. IEEE, 2023.
- Gen Luo, Ganlin Yang, Ziyang Gong, Guanzhou Chen, Haonan Duan, Erfei Cui, Ronglei Tong, Zhi Hou, Tianyi Zhang, Zhe Chen, et al. Visual embodied brain: Let multimodal large language models see, think, and control in spaces. *arXiv preprint arXiv:2506.00123*, 2025.
- Qi Lv, Weijie Kong, Hao Li, Jia Zeng, Zherui Qiu, Delin Qu, Haoming Song, Qizhi Chen, Xiang Deng, and Jiangmiao Pang. F1: A vision-language-action model bridging understanding and generation to actions. *arXiv preprint arXiv:2509.06951*, 2025.
- Kun Ouyang, Yuanxin Liu, Haoning Wu, Yi Liu, Hao Zhou, Jie Zhou, Fandong Meng, and Xu Sun. Spacer: Reinforcing mllms in video spatial reasoning. *arXiv preprint arXiv:2504.01805*, 2025.
- Abby O’Neill, Abdul Rehman, Abhiram Maddukuri, Abhishek Gupta, Abhishek Padalkar, Abraham Lee, Acorn Pooley, Agrim Gupta, Ajay Mandlekar, Ajinkya Jain, et al. Open

- x-embodiment: Robotic learning datasets and rt-x models: Open x-embodiment collaboration 0. In *2024 IEEE International Conference on Robotics and Automation (ICRA)*, pages 6892–6903. IEEE, 2024.
- William Peebles and Saining Xie. Scalable diffusion models with transformers. In *Proceedings of the IEEE/CVF international conference on computer vision*, pages 4195–4205, 2023.
- Karl Pertsch, Kyle Stachowicz, Brian Ichter, Danny Driess, Suraj Nair, Quan Vuong, Oier Mees, Chelsea Finn, and Sergey Levine. Fast: Efficient action tokenization for vision-language-action models. *arXiv preprint arXiv:2501.09747*, 2025.
- Delin Qu, Haoming Song, Qizhi Chen, Zhaoqing Chen, Xianqiang Gao, Xinyi Ye, Qi Lv, Modi Shi, Guanghui Ren, Cheng Ruan, Maoqing Yao, Haoran Yang, Jiacheng Bao, Bin Zhao, and Dong Wang. Eo-1: Interleaved vision-text-action pretraining for general robot control. *arXiv preprint*, 2025a. URL <https://arxiv.org/abs/2508.21112>.
- Delin Qu, Haoming Song, Qizhi Chen, Zhaoqing Chen, Xianqiang Gao, Xinyi Ye, Qi Lv, Modi Shi, Guanghui Ren, Cheng Ruan, et al. Eo-1: Interleaved vision-text-action pretraining for general robot control. *arXiv preprint arXiv:2508.21112*, 2025b.
- Delin Qu, Haoming Song, Qizhi Chen, Yuanqi Yao, Xinyi Ye, Yan Ding, Zhigang Wang, JiaYuan Gu, Bin Zhao, Dong Wang, et al. Spatialvla: Exploring spatial representations for visual-language-action model. *arXiv preprint arXiv:2501.15830*, 2025c.
- Vignesh Ramanathan, Anmol Kalia, Vladan Petrovic, Yi Wen, Baixue Zheng, Baishan Guo, Rui Wang, Aaron Marquez, Rama Kovvuri, Abhishek Kadian, et al. Paco: Parts and attributes of common objects. In *Proceedings of the IEEE/CVF Conference on Computer Vision and Pattern Recognition*, pages 7141–7151, 2023.
- Bytedance Seed. Seed1. 8 model card: Towards generalized real-world agency. Technical report, 2025a. Technical Report.
- Pierre Sermanet, Tianli Ding, Jeffrey Zhao, Fei Xia, Debidatta Dwibedi, Keerthana Gopalakrishnan, Christine Chan, Gabriel Dulac-Arnold, Sharath Maddineni, Nikhil J Joshi, et al. Robovqa: Multimodal long-horizon reasoning for robotics. In *2024 IEEE International Conference on Robotics and Automation (ICRA)*, pages 645–652. IEEE, 2024.
- Zhihong Shao, Peiyi Wang, Qihao Zhu, Runxin Xu, Junxiao Song, Xiao Bi, Haowei Zhang, Mingchuan Zhang, YK Li, Yang Wu, et al. Deepseekmath: Pushing the limits of mathematical reasoning in open language models. *arXiv preprint arXiv:2402.03300*, 2024.
- Chan Hee Song, Valts Blukis, Jonathan Tremblay, Stephen Tyree, Yu Su, and Stan Birchfield. Robospacial: Teaching spatial understanding to 2d and 3d vision-language models for robotics. In *Proceedings of the Computer Vision and Pattern Recognition Conference*, pages 15768–15780, 2025a.
- Wenxuan Song, Ziyang Zhou, Han Zhao, Jiayi Chen, Pengxiang Ding, Haodong Yan, Yuxin Huang, Feilong Tang, Donglin Wang, and Haoang Li. Reconvla: Reconstructive vision-language-action model as effective robot perceiver. *arXiv preprint arXiv:2508.10333*, 2025b.
- starVLA Contributors. Starvla: A lego-like codebase for vision-language-action model developing. GitHub repository, 1 2025. URL <https://github.com/starVLA/starVLA>.
- Gemini Robotics Team, Saminda Abeyruwan, Joshua Ainslie, Jean-Baptiste Alayrac, Montserrat Gonzalez Arenas, Travis Armstrong, Ashwin Balakrishna, Robert Baruch, Maria Bauza, Michiel Blokzijl, et al. Gemini robotics: Bringing ai into the physical world. *arXiv preprint arXiv:2503.20020*, 2025.
- Octo Model Team, Dibya Ghosh, Homer Walke, Karl Pertsch, Kevin Black, Oier Mees, Sudeep Dasari, Joey Hejna, Tobias Kreiman, Charles Xu, et al. Octo: An open-source generalist robot policy. *arXiv preprint arXiv:2405.12213*, 2024.
- Peter Tong, Ellis Brown, Penghao Wu, Sanghyun Woo, Adithya Jairam Vedagiri IYER, Sai Charitha Akula, Shusheng Yang, Jihan Yang, Manoj Middepogu, Ziteng Wang, et al. Cambrian-1: A fully open, vision-centric exploration of multimodal llms. *Advances in Neural Information Processing Systems*, 37:87310–87356, 2024.
- Weiyun Wang, Zhangwei Gao, Lixin Gu, Hengjun Pu, Long Cui, Xingguang Wei, Zhaoyang Liu, Linglin Jing, Shenglong Ye, Jie Shao, et al. Internvl3. 5: Advancing open-source multimodal models in versatility, reasoning, and efficiency. *arXiv preprint arXiv:2508.18265*, 2025a.
- Yuqi Wang, Xinghang Li, Wenxuan Wang, Junbo Zhang, Yingyan Li, Yuntao Chen, Xinlong Wang, and Zhaoxiang Zhang. Unified vision-language-action model. *arXiv preprint arXiv:2506.19850*, 2025b.

- Jason Wei, Xuezhi Wang, Dale Schuurmans, Maarten Bosma, Fei Xia, Ed Chi, Quoc V Le, Denny Zhou, et al. Chain-of-thought prompting elicits reasoning in large language models. *Advances in neural information processing systems*, 35:24824–24837, 2022.
- Junjie Wen, Yichen Zhu, Jinming Li, Minjie Zhu, Zhibin Tang, Kun Wu, Zhiyuan Xu, Ning Liu, Ran Cheng, Chaomin Shen, et al. Tinyvla: Towards fast, data-efficient vision-language-action models for robotic manipulation. *IEEE Robotics and Automation Letters*, 2025.
- Chenyuan Wu, Pengfei Zheng, Ruiran Yan, Shitao Xiao, Xin Luo, Yueze Wang, Wanli Li, Xiyang Jiang, Yexin Liu, Junjie Zhou, Ze Liu, Ziyi Xia, Chaofan Li, Haoge Deng, Jiahao Wang, Kun Luo, Bo Zhang, Defu Lian, Xinlong Wang, Zhongyuan Wang, Tiejun Huang, and Zheng Liu. Omnigen2: Exploration to advanced multimodal generation. *arXiv preprint arXiv:2506.18871*, 2025a.
- Kun Wu, Chengkai Hou, Jiaming Liu, Zhengping Che, Xiaozhu Ju, Zhuqin Yang, Meng Li, Yinuo Zhao, Zhiyuan Xu, Guang Yang, et al. Robomind: Benchmark on multi-embodiment intelligence normative data for robot manipulation. *arXiv preprint arXiv:2412.13877*, 2024.
- Shihan Wu, Xuecheng Liu, Shaoxuan Xie, Pengwei Wang, Xinghang Li, Bowen Yang, Zhe Li, Kai Zhu, Hongyu Wu, Yiheng Liu, et al. Robocoin: An open-sourced bimanual robotic data collection for integrated manipulation. *arXiv preprint arXiv:2511.17441*, 2025b.
- Wei Wu, Fan Lu, Yunnan Wang, Shuai Yang, Shi Liu, Fangjing Wang, Shuailei Ma, He Sun, Yong Wang, Zhenqi Qiu, Houlong Xiong, Ziyu Wang, Shuai Zhou, Yiyu Ren, Kejia Zhang, Hui Yu, Jingmei Zhao, Qian Zhu, Ran Cheng, Yong-Lu Li, Yongtao Huang, Xing Zhu, Yujun Shen, and Kecheng Zheng. A pragmatic vla foundation model. *arXiv preprint arXiv:2601.18692v1*, 2026.
- Tencent Robotics X and HY Vision Team. Hy-embodied-0.5: Embodied foundation models for real-world agents. *arXiv preprint arXiv:2604.07430*, 2026.
- Enze Xie, Junsong Chen, Junyu Chen, Han Cai, Haotian Tang, Yujun Lin, Zhekai Zhang, Muyang Li, Ligeng Zhu, Yao Lu, et al. Sana: Efficient high-resolution image synthesis with linear diffusion transformers. *arXiv preprint arXiv:2410.10629*, 2024.
- An Yang, Anfeng Li, Baosong Yang, Beichen Zhang, Binyuan Hui, Bo Zheng, Bowen Yu, Chang Gao, Chengen Huang, Chenxu Lv, et al. Qwen3 technical report. *arXiv preprint arXiv:2505.09388*, 2025a.
- Ganlin Yang, Tianyi Zhang, Haoran Hao, Weiyun Wang, Yibin Liu, Dehui Wang, Guanzhou Chen, Zijian Cai, Junting Chen, Weijie Su, et al. Vlaser: Vision-language-action model with synergistic embodied reasoning. *arXiv preprint arXiv:2510.11027*, 2025b.
- Jianwei Yang, Reuben Tan, Qianhui Wu, Ruijie Zheng, Baolin Peng, Yongyuan Liang, Yu Gu, Mu Cai, Seonghyeon Ye, Joel Jang, et al. Magma: A foundation model for multimodal ai agents. In *Proceedings of the computer vision and pattern recognition conference*, pages 14203–14214, 2025c.
- Jihan Yang, Shusheng Yang, Anjali Gupta, Rilyn Han, Li Fei-Fei, and Saining Xie. Thinking in Space: How Multimodal Large Language Models See, Remember and Recall Spaces. *arXiv preprint arXiv:2412.14171*, 2024.
- Rui Yang, Ziyu Zhu, Yanwei Li, Jingjia Huang, Shen Yan, Siyuan Zhou, Zhe Liu, Xiangtai Li, Shuangye Li, Wenqian Wang, et al. Visual spatial tuning. *arXiv preprint arXiv:2511.05491*, 2025d.
- Shusheng Yang, Jihan Yang, Pinzhi Huang, Ellis Brown, Zihao Yang, Yue Yu, Shengbang Tong, Zihan Zheng, Yifan Xu, Muhan Wang, Daohan Lu, Rob Fergus, Yann LeCun, Li Fei-Fei, and Saining Xie. Cambrian-s: Towards spatial supersensing in video. *arXiv preprint arXiv:2511.04670*, 2025e.
- Sihan Yang, Runsen Xu, Yiman Xie, Sizhe Yang, Mo Li, Jingli Lin, Chenming Zhu, Xiaochen Chen, Haodong Duan, Xiangyu Yue, et al. Mmsi-bench: A benchmark for multi-image spatial intelligence. *arXiv preprint arXiv:2505.23764*, 2025f.
- Junliang Ye, Zhengyi Wang, Ruowen Zhao, Shenghao Xie, and Jun Zhu. Shapellm-omni: A native multimodal llm for 3d generation and understanding. *arXiv preprint arXiv:2506.01853*, 2025.
- Chandan Yeshwanth, Yueh-Cheng Liu, Matthias Nießner, and Angela Dai. Scannet++: A high-fidelity dataset of 3d indoor scenes. In *Proceedings of the IEEE/CVF International Conference on Computer Vision*, pages 12–22, 2023.
- Baiqiao Yin, Qineng Wang, Pingyue Zhang, Jianshu Zhang, Kangrui Wang, Zihan Wang, Jieyu Zhang, Keshigeyan Chandrasegaran, Han Liu, Ranjay Krishna, et al. Spatial mental modeling from limited views. In *Structural Priors for Vision Workshop at ICCV'25*, 2025.

- Tianyuan Yuan, Yicheng Liu, Chenhao Lu, Zhuoguang Chen, Tao Jiang, and Hang Zhao. Depthvla: Enhancing vision-language-action models with depth-aware spatial reasoning. *arXiv preprint arXiv:2510.13375*, 2025a.
- Wentao Yuan, Jiafei Duan, Valts Blukis, Wilbert Pumacay, Ranjay Krishna, Adithyavairavan Murali, Arsalan Mousavian, and Dieter Fox. Robopoint: A vision-language model for spatial affordance prediction for robotics. *arXiv preprint arXiv:2406.10721*, 2024.
- Yifu Yuan, Haiqin Cui, Yaoting Huang, Yibin Chen, Fei Ni, Zibin Dong, Pengyi Li, Yan Zheng, and Jianye Hao. Embodied-r1: Reinforced embodied reasoning for general robotic manipulation. *arXiv preprint arXiv:2508.13998*, 2025b.
- Yanjie Ze, Gu Zhang, Kangning Zhang, Chenyuan Hu, Muhan Wang, and Huazhe Xu. 3d diffusion policy: Generalizable visuomotor policy learning via simple 3d representations. *arXiv preprint arXiv:2403.03954*, 2024.
- Jiahui Zhang, Yurui Chen, Yanpeng Zhou, Yueming Xu, Ze Huang, Jilin Mei, Junhui Chen, Yu-Jie Yuan, Xinyue Cai, Guowei Huang, et al. From flatland to space: Teaching vision-language models to perceive and reason in 3d. *arXiv preprint arXiv:2503.22976*, 2025a.
- Jianke Zhang, Yanjiang Guo, Yucheng Hu, Xiaoyu Chen, Xiang Zhu, and Jianyu Chen. Up-vla: A unified understanding and prediction model for embodied agent. *arXiv preprint arXiv:2501.18867*, 2025b.
- Wenyao Zhang, Hongsi Liu, Zekun Qi, Yunan Wang, Xinqiang Yu, Jiazhao Zhang, Runpei Dong, Jiawei He, He Wang, Zhizheng Zhang, Li Yi, Wenjun Zeng, and Xin Jin. Dreamvla: A vision-language-action model dreamed with comprehensive world knowledge. *CoRR*, abs/2507.04447, 2025c. <https://doi.org/10.48550/ARXIV.2507.04447>. URL <https://doi.org/10.48550/arXiv.2507.04447>.
- Yi Zhang, Che Liu, Xiancong Ren, Hanchu Ni, Shuai Zhang, Zeyuan Ding, Jiayu Hu, Hanzhe Shan, Zhenwei Niu, Zhaoyang Liu, et al. Pelican-vl 1.0: A foundation brain model for embodied intelligence. *arXiv preprint arXiv:2511.00108*, 2025d.
- Qingqing Zhao, Yao Lu, Moo Jin Kim, Zipeng Fu, Zhuoyang Zhang, Yecheng Wu, Zhaoshuo Li, Qianli Ma, Song Han, Chelsea Finn, et al. Cot-vla: Visual chain-of-thought reasoning for vision-language-action models. In *Proceedings of the Computer Vision and Pattern Recognition Conference*, pages 1702–1713, 2025a.
- Ruowen Zhao, Zhengyi Wang, Yikai Wang, Zihan Zhou, and Jun Zhu. Flexidreamer: Single image-to-3d generation with flexicubes. *arXiv preprint arXiv:2404.00987*, 2024.
- Ruowen Zhao, Junliang Ye, Zhengyi Wang, Guangce Liu, Yiwen Chen, Yikai Wang, and Jun Zhu. Deepmesh: Auto-regressive artist-mesh creation with reinforcement learning. In *Proceedings of the IEEE/CVF International Conference on Computer Vision*, pages 10612–10623, 2025b.
- Haoyu Zhen, Xiaowen Qiu, Peihao Chen, Jincheng Yang, Xin Yan, Yilun Du, Yining Hong, and Chuang Gan. 3d-vla: A 3d vision-language-action generative world model. *arXiv preprint arXiv:2403.09631*, 2024.
- Ruijie Zheng, Yongyuan Liang, Shuaiyi Huang, Jianfeng Gao, Hal Daumé III, Andrey Kolobov, Furong Huang, and Jianwei Yang. Tracevla: Visual trace prompting enhances spatial-temporal awareness for generalist robotic policies. *arXiv preprint arXiv:2412.10345*, 2024.
- Enshen Zhou, Jingkun An, Cheng Chi, Yi Han, Shanyu Rong, Chi Zhang, Pengwei Wang, Zhongyuan Wang, Tiejun Huang, Lu Sheng, et al. Roborefer: Towards spatial referring with reasoning in vision-language models for robotics. *arXiv preprint arXiv:2506.04308*, 2025.
- Qian-Yi Zhou, Jaesik Park, and Vladlen Koltun. Open3d: A modern library for 3d data processing. *arXiv preprint arXiv:1801.09847*, 2018.

Appendix

A SimplerEnv Evaluation on WidowX Robot Tasks

We further evaluate our approach in the SimplerEnv simulation environment Li et al. (2024b), specifically under the WidowX robot setup. The Simpler WidowX benchmark comprises four task suites, including *Put Carrot on Plate*, *Put Eggplant in Basket*, *Put Spoon on Towel* and *Stack Blocks*, which are designed to assess robustness to visual variations and precise manipulation. Following the StarVLA implementation starVLA Contributors (2025), we fine-tune GEM and its action expert from scratch on BridgeDataV2 O’Neill et al. (2024) for 50k steps. We report the final success rate for each task suite, which is evaluated over 100 trials with different random seeds. For a comprehensive comparison, we benchmark our method against both standard VLAs Chi et al. (2025); Team et al. (2024); Intelligence et al. (2025b); Kim et al. (2024) and recent VLAs equipped with spatial priors Liu et al. (2025a); Yang et al. (2025b); Qu et al. (2025c); Zheng et al. (2024); Huang et al. (2025). As shown in Table 5, GEM-VLA achieves the highest average success rate overall, establishing a robust foundation for sim-to-real transfer. Notably, the GEM-based VLA outperforms the VLA built on the standard SFT model, suggesting that GEM’s geometric priors help capture fine-grained spatial relationships and enable reliable action prediction in manipulation tasks.

Table 5: **Success rates on the Simpler WidowX Robot benchmark.** The highest and second-highest accuracy values are highlighted in **bold** and underlined, respectively. The results show that GEM-VLA achieves the highest average performance across all task types.

Model	Put Carrot	Put Eggplant	Put Spoon	Stack Block	Average
Diffusion Policy Chi et al. (2025)	0%	0%	4.2%	0%	1.1%
Octo-Base Team et al. (2024)	8.3%	43.1%	12.5%	31.9%	16.0%
OpenVLA Kim et al. (2024)	0%	4.1%	0%	0%	1.0%
π_0 Intelligence et al. (2025b)	<u>55.8%</u>	79.2%	63.3%	21.3%	54.9%
RoboVLM Liu et al. (2025a)	25.0%	58.3%	29.2%	12.5%	31.3%
TraceVLA Zheng et al. (2024)	16.6%	65.0%	12.5%	16.6%	27.7%
SpatialVLA Qu et al. (2025c)	25.0%	100%	16.7%	62.5%	42.7%
ThinkAct Huang et al. (2025)	37.5%	70.8%	58.3%	8.7%	43.8%
Vlaser Yang et al. (2025b)	52.5%	<u>87.9%</u>	<u>76.6%</u>	43.3%	<u>65.1%</u>
Qwen3VL-SFT-VLA	44.0%	80.0%	82.0%	40.0%	61.5%
GEM-VLA (Ours)	58.0%	84.0%	82.0%	<u>44.0%</u>	67.0%

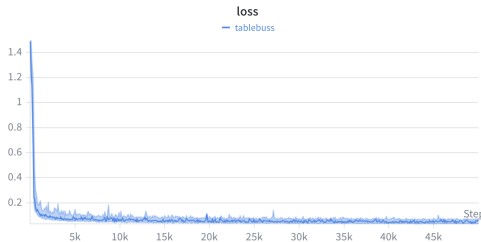
B More Implementation Details

Built on Qwen3-VL Bai et al. (2025) as the VLM backbone, GEM integrates a lightweight 2-layer MLP connector and a DiT-based depth generator to combine generative supervision with representation learning seamlessly. GEM achieves embodied capabilities through a progressive three-phase training strategy: (i) initialize the connector, (ii) initialize the depth generator, (iii) end-to-end joint training. Detailed training configurations, including hyperparameters and optimization settings, are reported in Table 6.

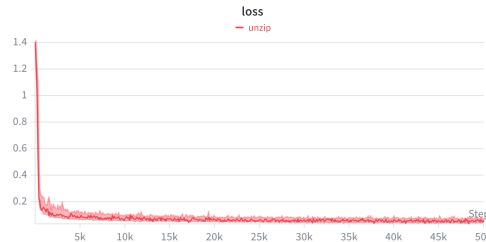
To enable real-world robotic task evaluation, we extend GEM with a flow-based action expert built on the RDT2 implementation Liu et al. (2026). For each specific task, we collect 200 trajectories and finetune the pretrained model for 50k steps with a global batch size of 256. We use an action chunk size of 32, and the observations consist of three camera views: one top view and two wrist views (left and right). The training loss curves are shown in Figure 6. Performance is evaluated using both progress score and overall success rate, and results are averaged over 50 runs for each task.

Table 6: Detailed configuration for each training stage in VLM pretraining of GEM.

Configurations	Stage 1	Stage 2	Stage 3
Batch Size	128	128	128
Learning Rate	1×10^{-3}	1×10^{-4}	1×10^{-5}
Training Steps	500 steps	4k steps	1 epoch
Optimizer	AdamW	AdamW	AdamW
Weight Decay	0.1	0.1	0.1
Warmup Ratio	0.00	0.00	0.03
LR Schedule	Cosine	Cosine	Cosine
Max Seq. Length	-	-	16384
GPU Num	32	32	32



(a) Loss curve on Table Bussing task.



(b) Loss curve on Unzipping task.

Fig. 6: Loss Curves of GEM-VLA on real-world task finetuning.

For comparison, we re-implement two baseline models, $\pi_{0.5}$ and π_0 -FAST, using the official OpenPI codebase. We train both baselines until convergence on 8 GPUs with a per-GPU batch size of 32. For $\pi_{0.5}$, we follow the official setup with discrete state inputs, an action horizon of 24, and a 32-dimensional action space. The training process uses bfloat16 precision and AdamW optimization. For π_0 -FAST implementation, we keep the optimizer and scheduler settings the same as $\pi_{0.5}$.

C Details on GEM-4M construction

C.1 Embodied Grounding Data

To further enhance grounding capabilities in physical manipulation scenarios, we generate an additional 100k high-quality data samples from open-source robot action datasets Wu et al. (2024); O’Neill et al. (2024); Khazatsky et al. (2024). The data generation process consists of two main stages. First, we extract the first frame of each robot operation video and employ Qwen3-VL Bai et al. (2025) to identify all object labels in its foreground, following the prompt templates provided in Figure 11. Next, we use SAM3 Carion et al. (2025) to obtain segmentation masks for each identified object label. To ensure annotation quality, only segmentation masks with confidence scores above 0.5 are retained. Since our annotations are in the form of bounding boxes or points, we derive bounding boxes by computing the minimum axis-aligned rectangle enclosing each mask, and obtain point annotations by randomly sampling a coordinate within the mask region. Some grounding examples are visualized in Figure 7.

C.2 Physical, Spatial Reasoning Data

To enhance spatial intelligence capabilities, we manually construct a dataset of 100k 3D spatial perception samples derived from ScanNet Dai et al. (2017), Scannet++ Yeshwanth et al. (2023) and ARKitScenes Baruch et al. (2021), following methodologies established in VSI-Bench Yang et al. (2024). Specifically, we first convert each raw scene mesh to an Open3D Zhou et al. (2018) point cloud and extract both spatial and semantic metadata from

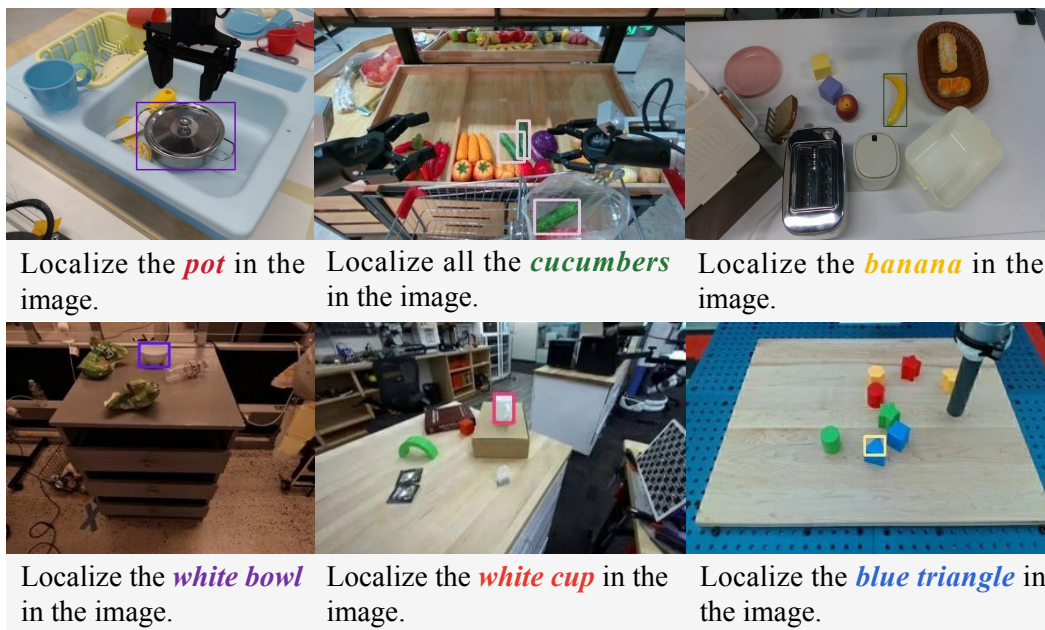


Fig. 7: **Embodied Grounding Examples.** The target objects mentioned in the instructions are localized in the scene and highlighted with bounding boxes.

the associated annotations. These include room dimensions, center coordinates, counts of object categories, and 3D bounding boxes with rotation, extents, and centers for each object instance. Based on these representations, we generate QA pairs about layout properties and inter-object relationships, covering object counts, absolute and relative distances, object and room sizes, relative directions, and other spatial attributes, following the VSI-Bench question templates. Some generated examples are visualized in Figure 8.

C.3 Spatiotemporal Planning Data

We collect robot videos from public datasets Wu et al. (2025b; 2024); Bu et al. (2025) with sub-task annotations and extract frames corresponding to each sub-task. Using these annotations, we generate question-answer pairs based on the RoboVQA Sermanet et al. (2024) template. Representative examples are shown in Figure 9.

We also generate trajectory data to help the model learn object motion and action execution. For each sub-task video clip, we identify the manipulated object from the sub-task description using Qwen3 Yang et al. (2025a) with the prompt templates in Figure 12. We then apply SAM3 Carion et al. (2025) to the initial frame to obtain an instance mask, and use the object centroid as the initial state for trajectory tracking Karaev et al. (2025). The resulting trajectory is smoothed with cubic spline interpolation, and six uniformly spaced points are sampled as the final visual trace. Representative Examples are shown in Figure 10.

D Limitation and Future Work

Although GEM achieves strong performance on a wide range of embodied recognition benchmarks and robotic manipulation tasks, there remains room to further scale the model in terms of model size and training data. Moreover, the current GEM-VLA architecture has not been pretrained on large-scale robot datasets. As future work, we plan to incorporate large-scale robot data pretraining to equip the model with richer physical knowledge and further evaluate and refine the proposed methods.



Fig. 8: **Spatial Reasoning Examples.** Examples of generated spatial QA pairs on diverse reasoning tasks, including absolute distance estimation, object size prediction, room-size estimation, and relative direction understanding.

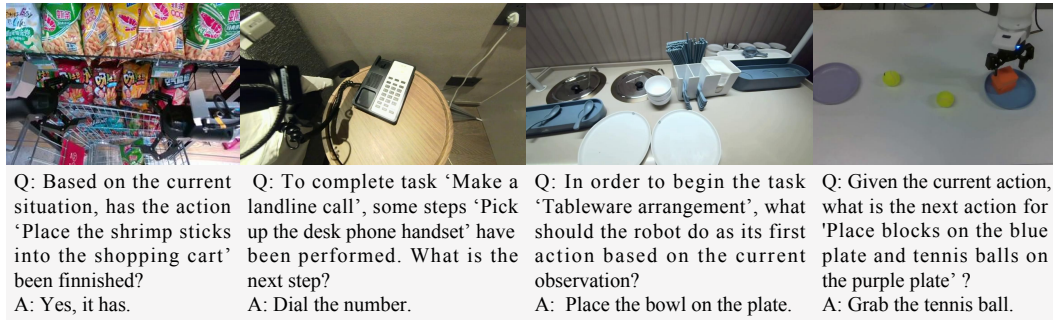


Fig. 9: **Planning Examples.** Examples of generated planning QA pairs, including task completion verification, next step prediction conditioned on current observation, and initial step prediction for complex tasks.

E Simulation Rollouts Visualization

In this section, we present qualitative visualizations of our model’s policy rollouts on simulation benchmarks. On LIBERO Liu et al. (2023a), we showcase successful rollouts on four representative manipulation tasks: LIBERO-Long, LIBERO-Goal, LIBERO-Object and LIBERO-Spatial in Figure 13. On SimplerEnv Li et al. (2024b) with the WidowX robot setup, we further present rollouts on four task suites: Put Carrot on Plate, Put Eggplant in Basket, Put Spoon on Towel and Stack Blocks in Figure 14. These qualitative results indicate that our model has strong potential for sim-to-real transfer.

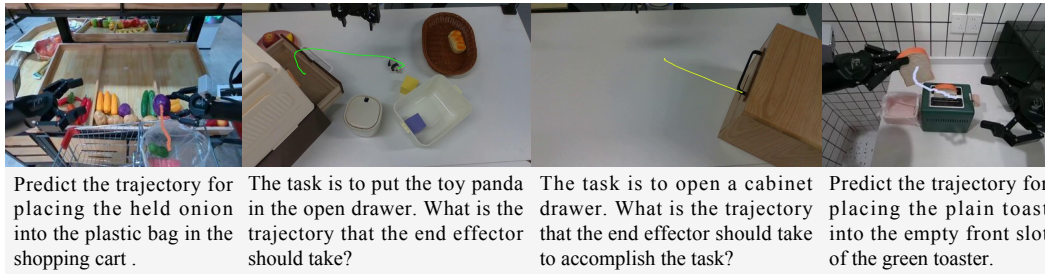


Fig. 10: **Trajectory Examples.** The trajectories, composed of key trajectory points, represent the model-predicted paths for task completion.

Prompt for Object Labels Extraction

Task
 First, identify and extract the objects mentioned in the instruction sentence. Then, based on the image, identify and list any additional objects that are clearly visible in the foreground or prominent areas of the image (such as on the table), excluding those already mentioned in the instruction sentence.

Extraction Rules

1. **Scope:** Extract the full noun phrase representing the object, including all descriptive modifiers (adjectives, colors, sizes) and quantifiers.
2. **Multiple Objects:** If there are multiple objects, list them in a comma-separated format.
3. **Foreground Focus:** Only include objects that are clearly visible in the foreground or main area of the image, such as on the table. Avoid including objects in the background or irrelevant items.

Output Format
 Return the objects as a JSON object with two keys:

- `instruction_mentioned_objects`: A list of objects mentioned in the instruction sentence.
- `additional_objects_in_image`: A list of objects visible in the image but not mentioned in the provided sentences.

Example
Input: Pick up the blue ring from the table and put it in the wooden tray
Output:

```
{
  "instruction_mentioned_objects": ["blue ring", "wooden tray"],
  "additional_objects_in_image": ["red ring", "green ring"]
}
```

Fig. 11: Prompt template for object labels extraction.

Prompt for Direct Object Extraction

Task
Extract the **direct object** (the entity being acted upon, manipulated, or moved) from the given instruction sentence.

Extraction Rules

1. Extract the full noun phrase representing the object, including all descriptive modifiers (adjectives, colors, sizes) and quantifiers.
2. Do not include verbs, prepositions (e.g., in, on, at), or destination/location (e.g., in “put apple on table”, extract only “apple”).
3. If no object is mentioned in the instruction, return “robot arm”.
4. If the instruction only mentions the action of the robot arm without specifying a manipulated object, return “robot arm”.
5. If the instruction mentions multiple objects being manipulated, return them separated by commas.

Output Format
Return only the extracted object text. Do not include punctuation, Markdown, or conversational filler.

Examples
Input: Drag strainer forwards.
Output: strainer
Input: Pick ketchup from table and place on oven.
Output: ketchup

Fig. 12: Prompt template for direct object extraction.

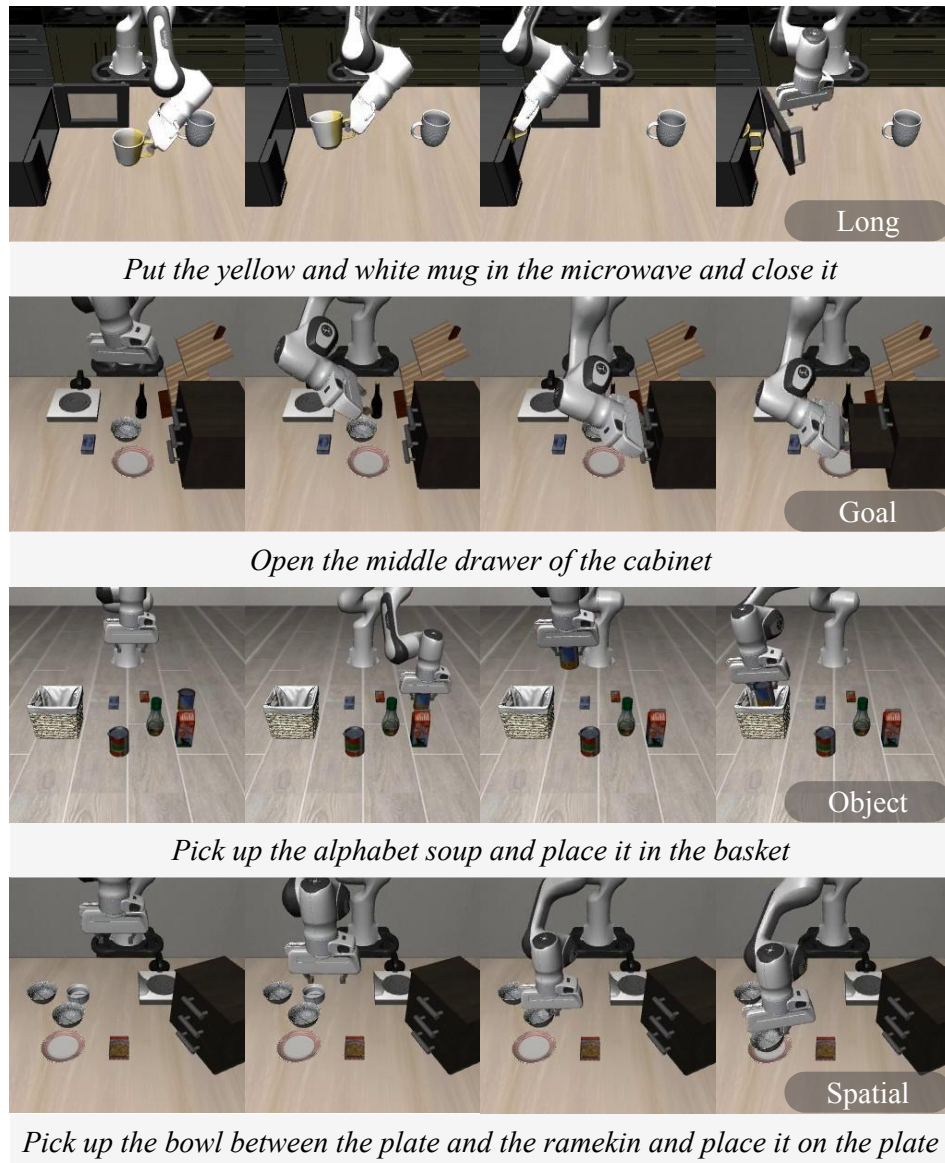


Fig. 13: Visualization of GEM-VLA's rollouts for LIBERO benchmark.

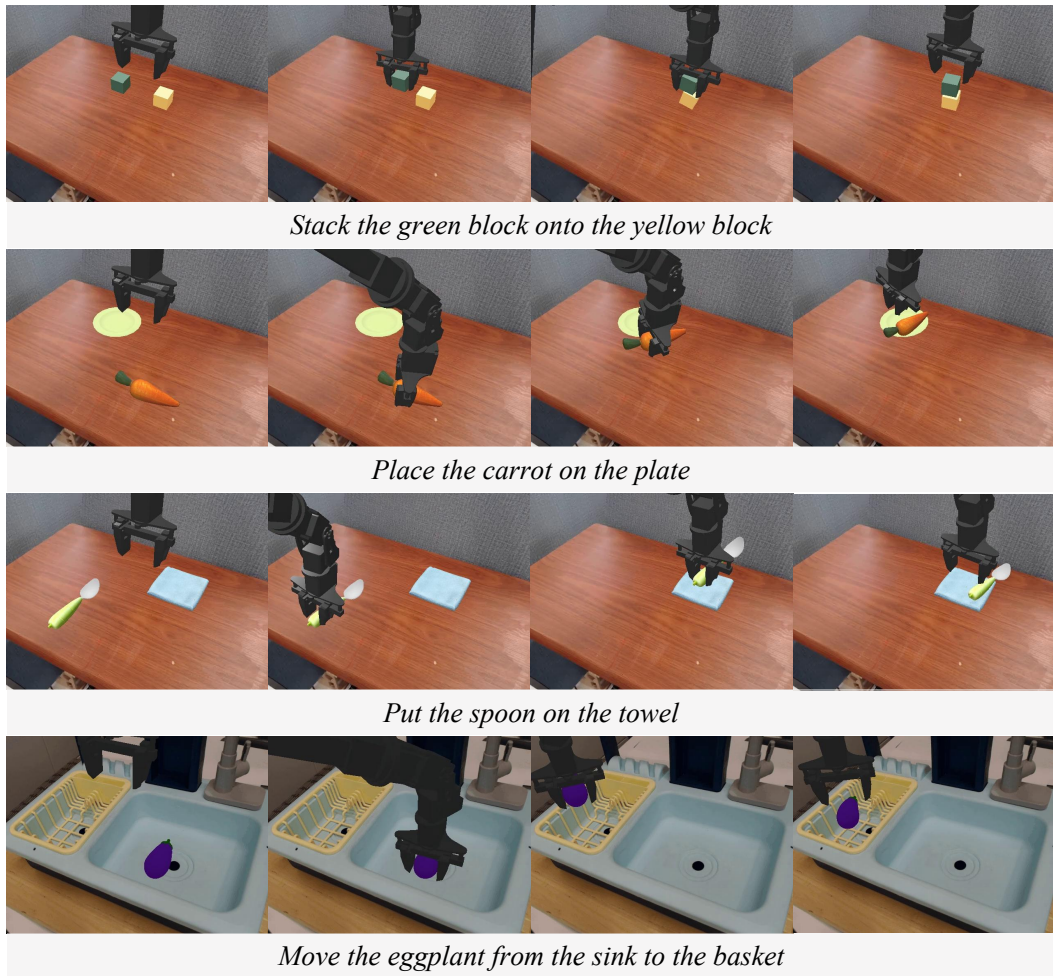


Fig. 14: Visualization of GEM-VLA's rollouts for Simpler WidowX benchmark.